

Effects of Extreme High Temperatures on Proliferation, Cell Cycle, Cell Differentiation and ROS of Adipose-Derived Mesenchymal Stromal Cells

Yuanhui Gao

Haikou Municipal People's Hospital and Xiangya Medical College Affiliated Hospital: Haikou Municipal People's Hospital and Central South University Xiangya Medical College Affiliated Hospital

Hui Cao

Haikou Municipal People's Hospital and Central South University Xiangya Medical College Affiliated Hospital

Shunlan Wang

Haikou Municipal People's Hospital and Central South University Xiangya Medical College Affiliated Hospital

Linlin Zheng

Haikou Municipal People's Hospital and Central South University Xiangya Medical College Affiliated Hospital

Haowei He

Haikou Municipal People's Hospital and Central South University Xiangya Medical College Affiliated Hospital

Zhenyu Nie

Haikou Municipal People's Hospital and Central South University Xiangya Medical College Affiliated Hospital

Mei Chen

Haikou Municipal People's Hospital and Central South University Xiangya Medical College Affiliated Hospital

Rong Jiang

Fujian Medical University

Denggao Huang (✉ hdg_qx@163.com)

Haikou Municipal People's Hospital and Xiangya Medical College Affiliated Hospital: Haikou Municipal People's Hospital and Central South University Xiangya Medical College Affiliated Hospital

<https://orcid.org/0000-0002-9927-1622>

Shufang Zhang

Haikou Municipal People's Hospital and Central South University Xiangya Medical College Affiliated Hospital

Research

Keywords: high temperature, adipose-derived mesenchymal stromal cells, proliferation, cell cycle, ROS

Posted Date: August 9th, 2021

DOI: <https://doi.org/10.21203/rs.3.rs-764300/v1>

License:  This work is licensed under a Creative Commons Attribution 4.0 International License.

[Read Full License](#)

1 **Effects of extreme high temperatures on proliferation, cell cycle, cell**
2 **differentiation and ROS of adipose-derived mesenchymal stromal**
3 **cells**

4 Yuanhui Gao¹, Hui Cao¹, Shunlan Wang¹, Linlin Zheng¹, Haowei He¹, Zhenyu Nie¹, Mei Chen¹,
5 Rong Jiang², Denggao Huang^{1#}, Shufang Zhang^{1#}

6
7 #Correspondence:

8 hdg_qx@163.com (Denggao Huang)

9 haikuoyiyuan@163.com (Shufang Zhang)

10 ¹Department of Central Laboratory, Afliated Haikou Hospital of Xiangya Medical College,
11 Central South University, Haikou 570208, Hainan, China

12 ²Department of General Surgery, 900th Hospital of the Joint Logistics Team/Clinical Institute of
13 Fuzhou General Hospital, Fujian Medical University/Dongfang Hospital Affiliated of Xiamen
14 University, Fuzhou 350025, Fujian, China

15
16 **Abstract**

17 **Backgrounds:** Global warming has led to extreme temperatures in different
18 latitudinal regions, resulting in the extinction of a large number of species. This study
19 focuses on the effects of extreme high temperatures on cell proliferation, cell cycle,
20 cell differentiation and mitochondria activity in human adipose-derived mesenchymal
21 stromal cells (hADSCs).

22 **Methods:** hADSCs were divided into three groups and incubated in 37°C, 39°C and
23 40°C environment for 5 hours of exposure each day, and then to 37°C circumstances
24 for further incubation. Cell surface markers, cell cycle, cell proliferation activity,
25 mitochondrial activity and cell polarization were detected and analyzed by flow
26 cytometry, CCK-8 assay, ROS and JC-1 staining respectively on the 1st and 3rd day of
27 cell culture; osteogenic and adipogenic differentiation ability of hASCs was analyzed
28 by staining after 21 days of osteogenic and adipogenic differentiation induction
29 culture.

30 **Results:** The results of this study showed that hASCs grown under high temperature
31 conditions had restricted growth activity, blocked S and G2 phases of the cell cycle,
32 reduced cytokinesis and impaired mitochondrial activity, while their osteogenic
33 differentiation ability and membrane potential depolarization were enhanced.

34 **Conclusions:** hADSCs were subjected to high temperature stimulation with restricted

35 growth activity, reduced cell division, impaired mitochondrial activity, significant cell
36 depolarization and enhanced osteogenic differentiation, and these results were closely
37 related to the pathogenic mechanisms of skin aging and heat stroke due to outdoor sun
38 exposure.

39 **Keywords:** high temperature; adipose-derived mesenchymal stromal cells;
40 proliferation; cell cycle; ROS

41

42 **Introduction**

43 Recently, global warming has led to extreme temperatures in different latitudinal
44 regions. Some studies have reported that high temperatures from temperate and
45 tropical regions may result in wildlife experiencing a dramatic increase in disease risk
46 ^[1]. As anthropogenic climate change continues to worsen, the risks to biodiversity will
47 increase over time, and future projections suggest that a potentially catastrophic
48 decline in global biodiversity is imminent ^[2], and these studies suggest that high
49 temperature environments pose a serious threat to both animals and people.

50 Previous reports have shown that high temperature radiation can cause skin aging
51 and slow down lipid metabolism. Ken Kobayashi et al ^[3] showed that lactating mice,
52 under moderately high temperature conditions at 39°C, induced higher lactation
53 capacity of mammary epithelial cells (MECs) through control of STAT5 and STAT3
54 signaling. In contrast, prolonged exposure to 41°C gave rise to a decrease in milk
55 production capacity through inactivation of STAT5 and a decrease in the total number
56 of MECs. It has also been shown that when rats are exposed to high temperature
57 (50°C), lipolysis in adipose tissue is inhibited due to their high body temperature,
58 while intravascular lipolysis is activated ^[4]. Therefore, understanding the response of
59 human cells to high temperature environment can help us to make positive responses
60 to future environmental changes.

61 With climate change, the increasing incidence of heat-related deaths has been a
62 frequent concern. The 2019 Global Burden of Disease, Injury, and Risk Factors Study
63 demonstrates the non-optimal temperature as one of the top 10 causes of death
64 globally. Globally, 5 million deaths from 2000 to 2019 are associated with abnormal
65 temperatures ^[6]. For example, a common illness, heat stroke (HS) is a life- threatening
66 disease defined as exposure to excessive hyperthermia at core temperatures above
67 40°C and resulting in a systemic inflammatory response syndrome ^[7]. HS occurs

68 when multiple tissues and organs are damaged, allowing the secretion of
69 pro-inflammatory cytokines including tumor necrosis factor- α (TNF- α) and
70 interleukin-6 (IL-6), and ultimately systemic inflammation ^[8]. However, the specific
71 pathogenic mechanisms need to be further investigated.

72 Adipose tissue is a highly metabolically active endocrine organ, which plays an
73 important role in energy storage, energy balance and metabolic regulation ^[9].
74 However, many statistics in recent years have shown that body temperature in healthy
75 adults is gradually decreasing ^[10-11], suggesting that some changes in adipose tissue in
76 the body are occurring with environmental changes or induced. Therefore, studying
77 the changes in cellular properties in adipose tissue in abnormal environments will help
78 us better understand the effects of environmental changes on the human body.
79 Currently, there are fewer reports on the effects of high temperature environments on
80 adipocytes. The aim of this experiment is to analyze the changes in cell morphology,
81 cell phenotype, cell proliferation, cell differentiation, cell cycle, ROS and membrane
82 potential depolarization of hADSCs at 37°C - 40°C. The purpose of this study was to
83 analyze the effect of high temperature environment on the biological properties of
84 hADSCs.

85

86 **1 Materials and Methods**

87 **1.1 Materials**

88 Human adipose-derived mesenchymal stromal cells (#HUXMD-01001) and
89 human adipose-derived mesenchymal stromal cell medium (#HUXMD-90031) were
90 purchased from Cyagen Biosciences (Guangzhou). Dulbecco's Phosphate Buffer
91 Solution (D-PBS, #8119217) and Trypsin (#2177715) purchased from Gibco;
92 Antibodies of CD105-PE (#560839), CD73-PE (#550257), CD34-PE (#348057),
93 CD90-PE (#561970), CD45-PE (#557059) purchased from Becton, Dickinson and
94 Company (Guangzhou, China). Cell Counting Kit-8 kit (#SA616) was purchased from
95 Dojindo; ROS fluorescent probe Dihydroethidium-Hydroethidine (DHE, #D1008) and
96 Mitochondrial membrane-potential dye (JC-1, #J4001) were purchased from US
97 EVERBRIGHT, Inc.

98 **1.2 Methods**

99 **1.2.1 Cell culture and temperature exposure experiments**

100 To understand the effect of different temperatures on hADSCs cells. For the

101 experiment, Passage 4(P4) of hADSCs cells were adjusted to the appropriate cell
102 density and inoculated in 6-well plates. The cells were incubated in different
103 temperature (37°C, 39°C, 40°C) incubators for 5h every day, and the cells were
104 uniformly placed in the same temperature incubator at 37°C after the end of
105 stimulation, then the cell morphology was then observed and photographed. The
106 duration of continuous treatment ranged from 1-28d depending on the design of the
107 different experiments.

108 **1.2.2 Cell surface marker determination assay**

109 The cells treated with different temperatures were used to determine the
110 expression of hADSCs surface markers CD105-PE, CD90-PE, CD73-PE, CD34-PE
111 and CD45-PE by flow cytometry. The cells were first digested with 0.25% trypsin and
112 collected in suspension, the cell density was adjusted (1×10^5 cells/mL) and washed
113 twice with Dulbecco's Phosphate Buffer Solution (D-PBS); the cells were then
114 resuspended in D-PBS, centrifuged at 3000 rpm for 5 min, the supernatant was
115 discarded, the appropriate amount of fluorescently labeled monoclonal antibody was
116 added and incubated for 30 min at room temperature and protected from light. The
117 cells were resuspended with 300 μ L D-PBS and analyzed by BD FACSDIVA software,
118 and the surface antigen expression was expressed as a percentage (%).

119 **1.2.3 Cell Counting Kit-8 (CCK-8) assay**

120 When the stimulated cells reach the time point of the assay, aspirate all the
121 medium and add 200 μ L of fresh medium and 20 μ L of CCK-8 reagent (10%), then
122 incubate in the incubator for 1 to 4 h. At the time point, 100 μ L of supernatant
123 medium was taken into a 96-well plate and the optical density (OD) was read at 450
124 nm using an enzyme marker.

125 **1.2.4 Cell cycle assay**

126 The P4 cells were adjusted to 10^6 cells per tube and centrifuged at 250g for 5 min.
127 The supernatant was discarded, and the cells were fixed in 70% ethanol at 4°C for
128 more than 2 h and centrifuged at 250g for 5 min. 100 μ L of RNaseA was added to the
129 supernatant for 30 min in a water bath at 37°C. 400 μ L of PI stain was added and
130 mixed at 4°C for 30 min, protected from light. The cells were detected by FACScanto
131 6 flow cytometer and the percentage of cells in G0/G1, S and G2/M phases of the cell
132 cycle (%) was calculated.

133 **1.2.5 Osteogenic and lipogenic differentiation induction assay**

134 The hADSCs of P4 were inoculated into gelatinized 6-well plates. When the

135 cells were confluent to 60-70%, the osteogenic differentiation induction medium was
136 changed every 3 days, and after 2-4 weeks of induction, alizarin red staining was
137 performed; When the cells were confluent to 100%, they were replaced with lipogenic
138 differentiation induction medium solution A and after 3 days with lipogenic
139 differentiation induction medium solution B. After 24 h, solution B was aspirated and
140 solution A was added, and solution A and B were alternately induced 3-5 times, and
141 finally the culture was maintained with solution B for 4-7 days until the lipid droplets
142 became large and round enough for oil red O staining. After induction of
143 differentiation staining by both methods, 10 randomly selected fields of view were
144 photographed under high magnification using uniform photographic conditions. The
145 area of cells stained with red calcified nodules (osteogenic differentiation) or red lipid
146 droplets (lipogenic differentiation) and the area of all cells in the whole area
147 photographed were measured using Image J software, and the ratio of the area of
148 differentiated cells to the total area was calculated as the result and expressed as a
149 percentage (%).

150 **1.2.6 Reactive oxygen species (ROS) and JC-1 staining assay**

151 The hADSCs of P4 were stained with JC-1 dye and ROS probe to determine the
152 mitochondrial membrane potential and intracellular ROS content, respectively.
153 Staining was performed according to the instructions of the ROS Fluorescent
154 Probes-DHE and JC-1 kits. Diluted ROS probe solution (1 μ M) and JC-1 dye
155 (10 μ g/ml) were added to the cell well plates and incubated in an incubator at 37°C for
156 10-30min protected from light. After being washed twice with D-PBS, they were
157 observed under a fluorescent microscope and photographed. Cells with weak
158 mitochondrial activity stained red for ROS, while cells stained with JC-1 went from
159 red to green fluorescence, indicating a decrease in mitochondrial membrane potential.

160 **1.2.7 Statistical Analysis**

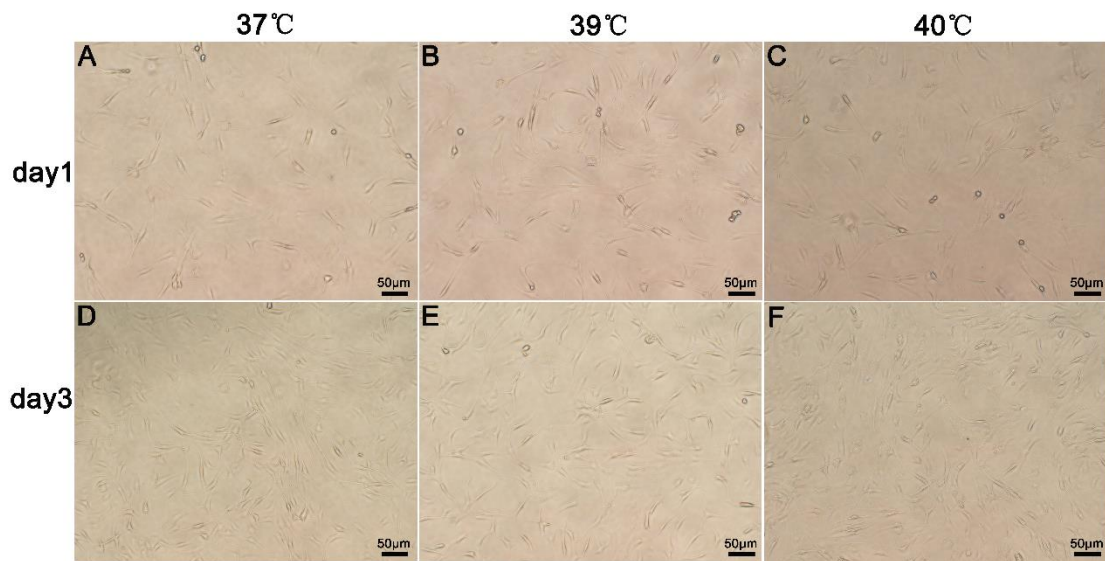
161 Data were reported as mean and standard error, and SPSS 22.0 and Data were
162 expressed as mean and standard error, and data were analyzed using IBM SPSS
163 Statistics 22.0 (IBM, USA) and plotted using Adobe Photoshop Cs5 (Adobe Systems
164 Inc, USA) and GraphPad prism 7 (GraphPad Software, USA). Differences and
165 significance were verified by one-way ANOVA. A p value <0.05 was considered as
166 statistically significant.

167

168 **2 Results**

169 **2.1 Cell morphology of hADSCs**

170 The cell morphology of hADSCs was observed under different temperature
171 gradient treatments, and no morphological differences were observed in hADSCs on
172 the 1st day (Fig 1). When the cells grew to the 3rd day, the cells in the 37°C group
173 showed a gradual swirling growth trend, while the cells in the 39°C group showed a
174 scattered growth. vacuole-like changes were seen in the cytoplasm of the cells in the
175 40°C group.



176

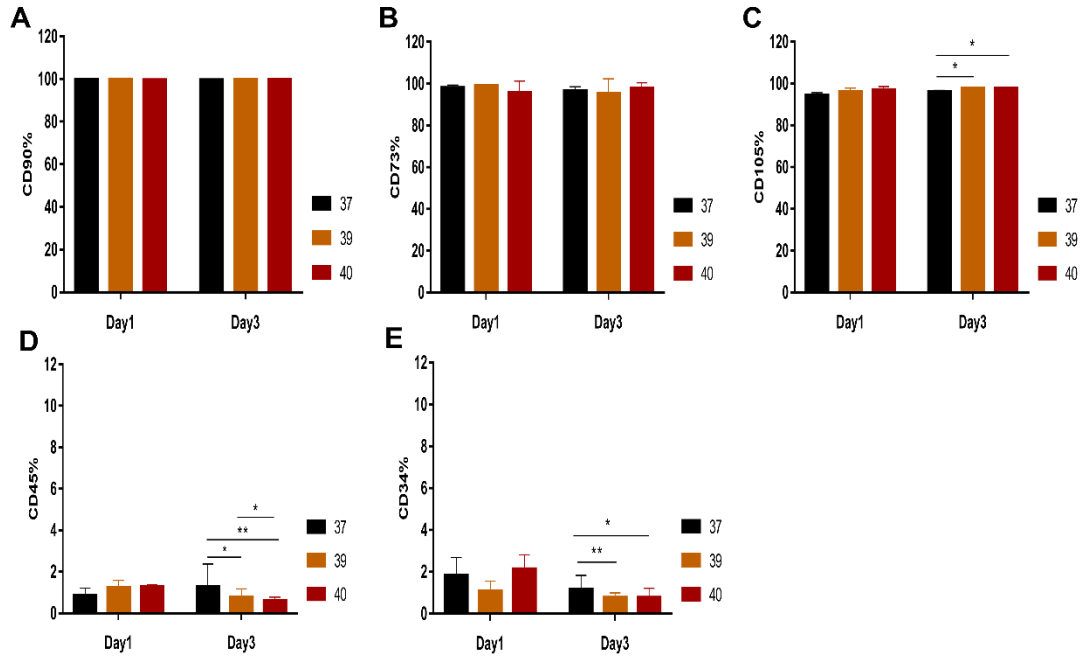
177 Fig1. Cell morphological characteristics of hADSCs in different temperature treatment groups.

178 A-C were the cell morphology of the 1st day in the 37°C, 39°C and 40°C groups, respectively, and

179 D-F were the cell morphology of the 3rd day in each group.

180 **2.2 Cell surface markers of hADSCs**

181 To understand whether the phenotype of hADSCs changed after different
182 temperature exposures, we performed flow cytometric assays on cell surface markers
183 of hADSCs treated at 37°C, 39°C and 40°C groups, respectively. The results showed
184 that CD90, CD73 and CD105 expression rates were above 90%, while CD34 and
185 CD45 expression rates were <3% (Fig 2). Statistical analysis showed that CD90 and
186 CD73 were not statistically different between groups on the 1st day and the 3rd day,
187 CD105 expression increased with increasing temperature on the 3rd day ($P<0.5$), and
188 CD34 and CD45 expression decreased with increasing temperature on the 3rd day
189 ($P<0.05$).

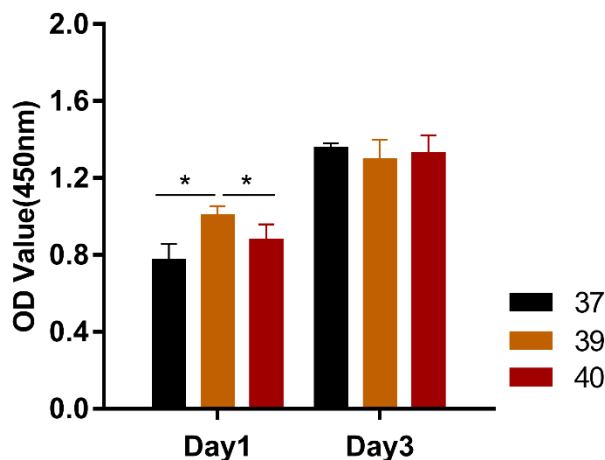


190

191 Fig2. Flow cytometry analysis of cell surface markers. hADSCs were positive for CD90, CD73,
 192 CD10 expression and negative for CD45 and CD34 expression. A-E indicates the percentage of
 193 each marker on the 1st day and the 3rd day after hADSCs were treated with different temperature
 194 groups, respectively. Values bar were expressed as mean±SEM, *P < 0.05, **P < 0.01.

195 2.3 Cell proliferation of hADSCs

196 This experiment used CCK-8 assay to analyze the proliferation viability of
 197 hADSCs at different temperatures (37°C, 39°C and 40°C group) by measuring the OD
 198 values of the cells. The results were shown in Figure 3: on the 1st day, hADSCs were
 199 significantly increased in the 39°C group compared with the other two groups
 200 (P<0.05); on the 3rd day, there was no statistical difference between the three groups.



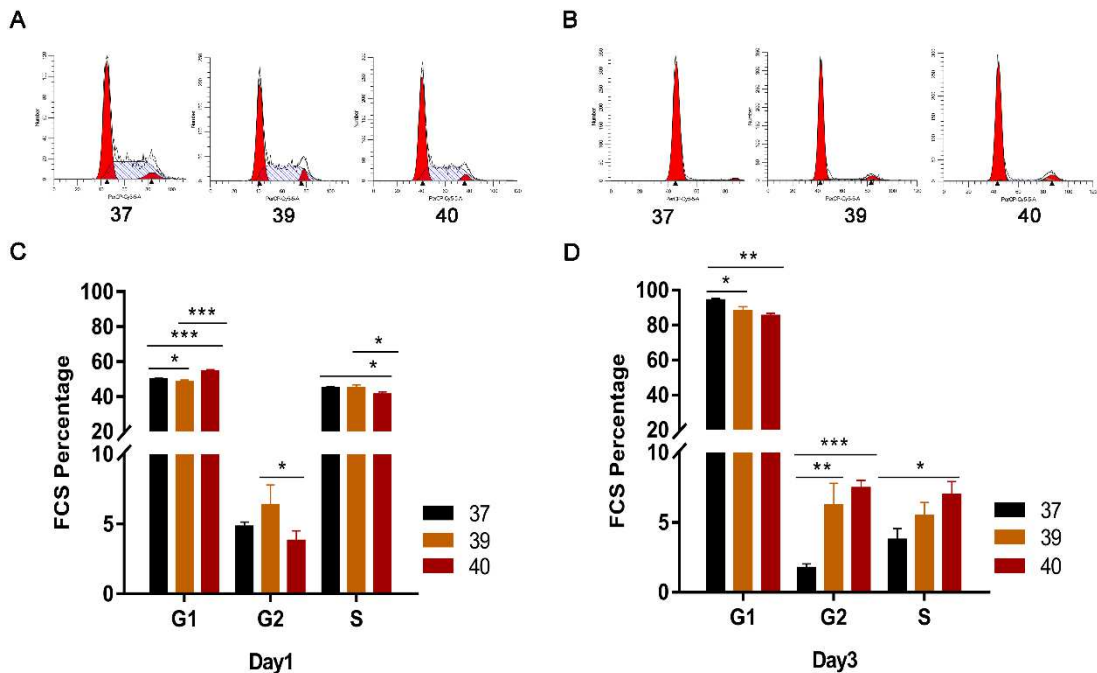
201

202 Fig3. Comparison of different temperature treatment groups on the proliferation of hADSCs.

203 Values bar were expressed as mean±SEM, *P < 0.05.

204 2.4 Cell cycle variation in hADSCs

205 The cell cycle of hADSCs in each group was measured by flow cytometry, and
206 the results showed (Fig 4) that at the 1st day, the proportion of cells in G1 phase was
207 greater in the 37°C group (50.01%±0.40%) than in the 39°C group (48.53%±
208 0.96%) and less than in the 40°C group (54.71%±0.61%), and the difference was
209 statistically significant; the proportion of cells in G2 phase was highest in the 39°C
210 group, which was significantly different from the 40°C group; the proportion of
211 S-phase of cells in both the 37°C and 39°C groups was greater than that in the 40°C
212 group. At the 3rd day, the G1 phase of all three groups increased compared with the 1st
213 day, and the proportion of G1 phase of cells gradually decreased with the increase of
214 temperature, while the proportion of G2 and S phases of cells gradually increased.



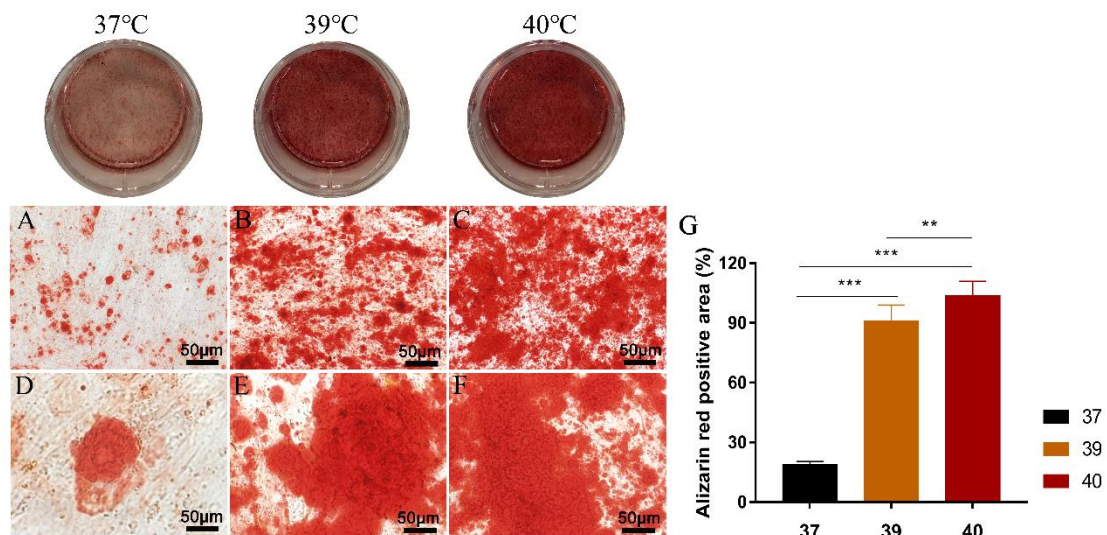
215

216 Fig4. Flow cytometry analysis of cell cycle. A and B represent scatter plots of the cell cycle of
217 hADSCs on the 1st day and the 3rd day after treatment with different temperature groups,
218 respectively. C and D represent histograms of the proportion of each phase of the cell cycle of
219 hADSCs on the 1st day and the 3rd day after treatment with different temperature groups,
220 respectively. Values bar were expressed as mean±SEM, *P < 0.05, **P < 0.01, ***P < 0.001.

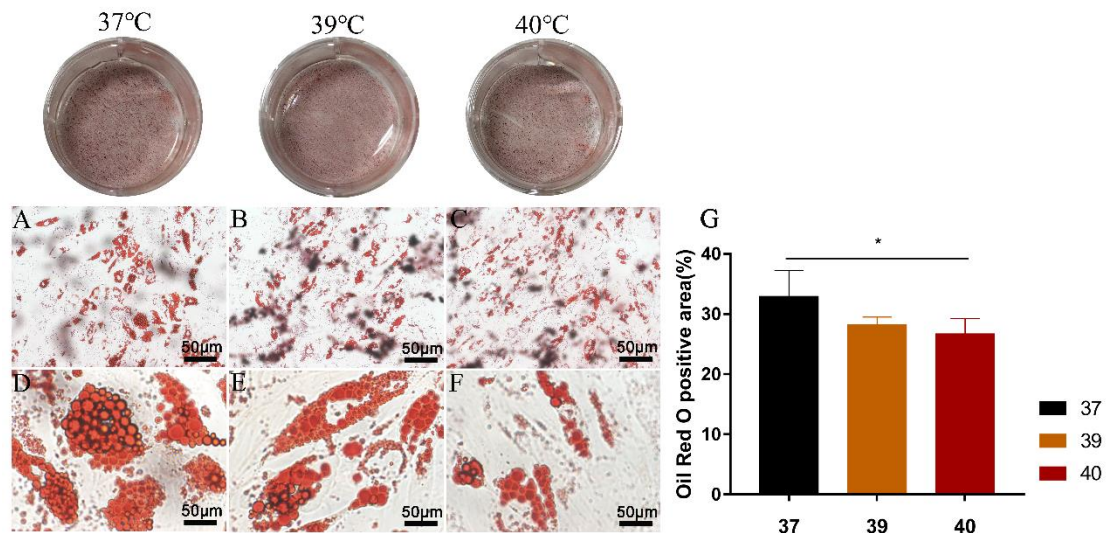
221 2.5 Osteogenic and lipogenic differentiation ability of hADSCs

222 After osteogenesis-induced differentiation of hADSCs from three different
223 temperature-stimulated groups, the formation of red calcified nodules was detected by
224 alizarin red staining, and microscopic observation showed that all three groups of cells

225 could form red calcified nodules to different degrees, and the rate of cellular calcium
 226 nodule formation increased with the increase of temperature (Fig5.A-F); as shown in
 227 the bar graph (Fig5.G), the trend of cellular calcium nodule formation was 37°C group
 228 (18.71 ± 1.73) < 39 °C group (91.03 ± 8.03) < 40 °C group (103.58 ± 7.32) ($P<0.01$).
 229 After lipogenesis-induced differentiation of hADSCs from three different temperature
 230 stimulation groups, they were stained with oil red O. Microscopic observation showed
 231 that all three groups of cells showed lipid droplets of different sizes (Fig6.A-F), the
 232 saturation of cellular lipid droplets decreased with increasing temperature, and the
 233 size of cellular lipid droplets showed 37°C group (32.90 ± 4.32) > 39°C group
 234 (28.19 ± 1.32) > 40°C group (26.69 ± 2.55), with a statistical difference between the
 235 37°C and 40°C groups.



236
 237 Fig5. Osteogenic differentiation potential of hADSCs after different temperature treatment. A-C
 238 were the results of alizarin red staining in the 37 °C group, 39 °C group and 40 °C group observed
 239 at low magnification, while D-F represent their results at high magnification, respectively. G was
 240 the quantification of alizarin red staining score. Values bar were expressed as mean±SEM, **P <
 241 0.01, ***P < 0.001.

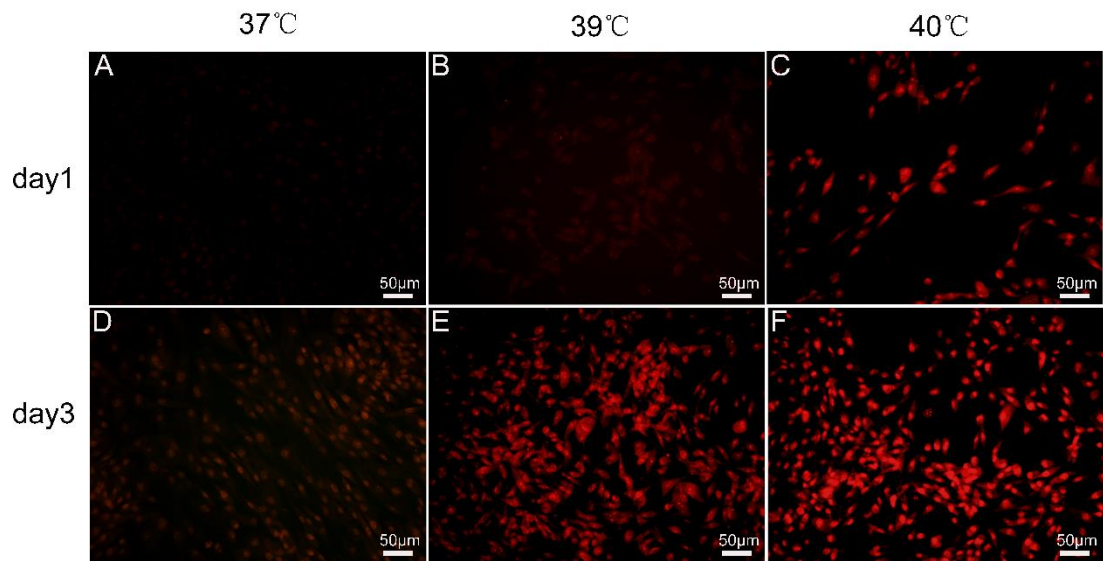


242

243 Fig6. Lipogenic differentiation potential of hADSCs after different temperature treatment. A-C
 244 were the results of oil-red O staining observed at low magnification for the 37 °C group, 39 °C
 245 group and 40 °C group, while D-F represent their results at high magnification, respectively. G
 246 was the quantification of oil-red O staining scores. Values bar were expressed as mean±SEM, *P <
 247 0.05.

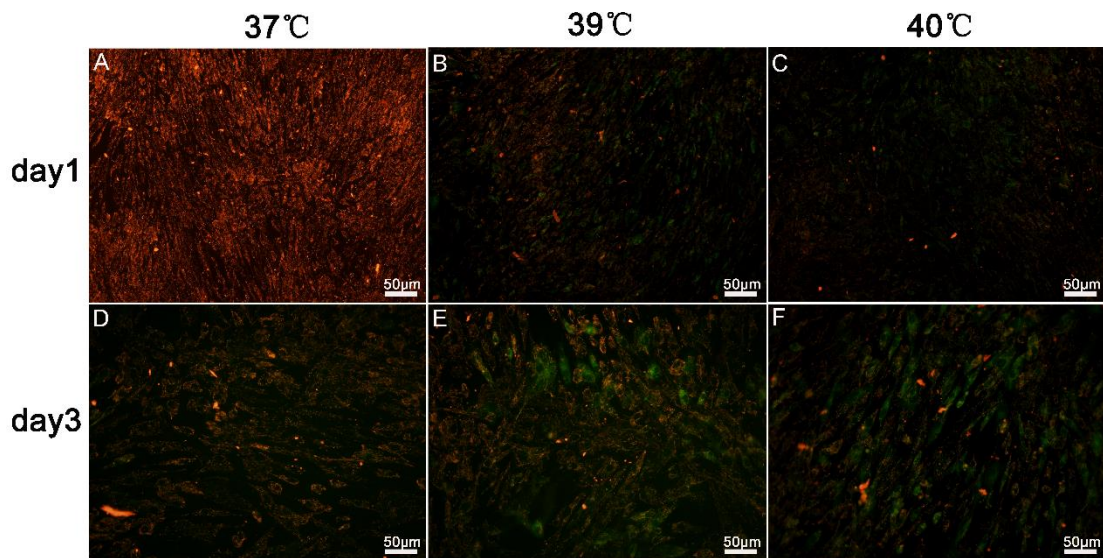
248 2.6 Results of ROS and JC-1 assay

249 The ROS content of hADSCs on the 1st day and the 3rd day after different
 250 temperature treatments in the three groups was measured by ROS probes. As shown in
 251 Fig 7, at the 1st day, the ROS fluorescence intensity was weak and not significantly
 252 different between the 37°C and 39°C groups, while the ROS fluorescence intensity
 253 was significantly enhanced in the high temperature (40°C) group; at the 3rd day, the
 254 fluorescence was still weak in the 37°C group, while the ROS fluorescence expression
 255 intensity was significantly enhanced in the 39°C and 40°C groups. The results of
 256 mitochondrial membrane potential measurement using JC-1 dye were shown in Figure
 257 8, which showed that the trend of mitochondrial membrane potential change was a
 258 gradual increase in membrane potential depolarization with the increase in ambient
 259 temperature. The effect of JC-1 membrane potential sensitive dye on mitochondrial
 260 depolarization was observed by fluorescence microscopy, with high potentials
 261 characterized by red fluorescence, while low potentials showed green fluorescence.
 262 The results showed that the depolarization was more pronounced at higher
 263 temperatures.



264

265 Fig7. Effect of different temperature groups on ROS content of hADSCs. A-C were the expression
 266 of ROS of hADSCs at the 1st day; D-F were the expression of ROS of hADSCs at the 3rd day.



267

268 Fig 8. Effect of different temperature groups on mitochondrial depolarization of hADSCs. A-C
 269 were the mitochondrial membrane potential changes of hADSCs at the 1st day; D-F were the
 270 mitochondrial membrane potential changes of hADSCs at the 3rd day.

271

272 **Discussion**

273 Global warming will affect ecosystems as well as human health in multiple ways,
 274 and these impacts are expected to rise dramatically with increasing warming, with
 275 estimates that the number of people at climate-related risk will increase by hundreds
 276 of millions by 2050. However, it remains difficult to predict the human impacts of the
 277 complex interplay of mechanisms driven by warming ^[12]. At present, the impact of
 278 climate warming on human survival and in animals is still poorly understood.

279 Yellow adipose tissue is mainly distributed in subcutaneous tissues, omentum
280 and mesentery, and is the largest energy reservoir in the body. It has the function of
281 storing fat, maintaining and regulating body temperature and participating in fat
282 metabolism ^[13]. There are more reports on how adipose tissue responds to changes in
283 the external environment at low temperatures, but few studies have examined the
284 changes in adipose tissue at high temperatures. In this study, we chose adipose-
285 derived human adipose mesenchymal stromal cells as the subject to explore the
286 biological properties of the cells and the changes in oxidative stress under high
287 temperature environment.

288 Available reports show that positive expression of CD73, CD105 and CD90, and
289 negative expression of CD34 and CD45 are cell surface markers of ADSCs ^[14,15]. To
290 clarify whether cell surface markers change at different temperatures exposure. This
291 study showed no significant changes from the cell morphology, but subtle differences
292 in their cell surface markers have been observed. At the 3rd day of treatment at
293 different temperatures, the expression of CD105 was increased at 39°C and 40°C
294 compared to 37°C, indicating an enhanced chondrogenic capacity ^[16]. In contrast, the
295 expression of CD34 and CD45 decreased and was <5%, suggesting that the cells still
296 have the characteristics of mesenchymal stromal cells ^[17]. Analysis of cell
297 proliferation viability showed that at 24 h after passaging, the proliferation capacity of
298 hADSCs in the 39°C environment was significantly higher than the other two groups,
299 and by 72 h, the proliferation capacity of cells in the 37°C group was slightly higher
300 than the others, showing that the change in environmental high temperature caused a
301 short-term rapid proliferation of hADSCs, while the opposite proliferation trend
302 occurred by 72 h. Further analysis in terms of cell cycle showed that at the 3rd day of
303 cell growth, the G1 phase (pre-DNA synthesis phase) was reduced and the S phase
304 (DNA replication phase) and G2 phase (late DNA synthesis phase) were significantly
305 higher in the 39°C and 40°C environments compared to the 37°C group, illustrating
306 that the S and G2 phases of the cells were blocked and the cell division ability was
307 reduced, which were consistent with the formation of a gradual decrease in cell
308 proliferation activity at the 3rd day.

309 The multidirectional differentiation potential of stromal cells is one of the
310 functions of stromal cells measured. This experiment showed that the rate of cellular
311 calcium nodule formation increased with increasing temperature after osteogenesis-
312 induced differentiation of hADSCs in each group, and the saturation of cellular lipid

313 droplets decreased with increasing temperature after lipogenesis-induced
314 differentiation. This indicates that temperature exerts an important influence on the
315 differentiation of stromal cells. Jang et al ^[18] compared the differences in indoor and
316 outdoor summer temperatures and humidity in Korea and Southeast Asia to assess
317 changes in skin studies showed that repeated exposure to high temperatures and high
318 humidity increased sebum content and hemoglobin index in human skin. However,
319 repeated temperature differences can relax skin blood vessels and reduce skin
320 elasticity, which can contribute to skin aging. These results were associated with a
321 greater tendency for cells to become chondrogenic and differentiated at elevated
322 temperatures. Kim et al ^[19] recruited 20 women aged 20 to 40 years. After exposing
323 them to outdoor and indoor environments for 90 minutes, skin assessments were
324 performed on the face (forehead and cheeks) and forearms to determine the degree of
325 skin hydration, sebum secretion, transepidermal water loss, pH, and oil content. The
326 study showed that hot environments produce more sweat, increase hydration, sebum
327 secretion, water loss, and lower skin pH. These results suggest that hot environments
328 produce varying degrees of disruption to human skin and to the function and
329 metabolism of epidermal cells. These results are relatively similar to the tendency of
330 hADSCs to osteogenic differentiation by high-temperature environments.

331 Proton pumps are present in the inner mitochondrial membrane and can pump
332 matrix protons into the membrane gap. Proton translocation across the membrane
333 allows the mitochondrial membrane gap to accumulate large internal amounts of
334 protons, described as a proton gradient: the mitochondrial membrane gap generates a
335 large positive charge while the mitochondrial matrix generates a large negative charge,
336 resulting in a transmembrane potential ($\Delta\Psi$) across the inner mitochondrial membrane,
337 referred to as the mitochondrial membrane potential. Normal mitochondrial
338 membrane potential is a prerequisite for maintaining oxidative phosphorylation and
339 ATP production in mitochondria and is necessary for maintaining mitochondrial
340 function, while an important change during apoptosis is the collapse of mitochondrial
341 membrane potential ^[20]. JC-1 is an ideal fluorescent probe widely used to detect
342 mitochondrial membrane electrical $\Delta\Psi_m$ sites. JC-1 dye accumulates within
343 mitochondria in a potential- dependent manner and can be used to detect cellular,
344 tissue or purified mitochondrial membrane potentials. In normal mitochondria, JC-1
345 aggregates in the mitochondrial matrix to form polymers, which emit intense red
346 fluorescence (Ex=585 nm, Em=590 nm); in unhealthy mitochondria, due to a decrease

347 or loss of membrane potential, JC-1 can only exist as a monomer in the cytoplasm,
348 producing green fluorescence (Ex=514 nm, Em=529 nm). JC-1 is not only used for
349 qualitative detection, because the change of color can reflect the change of
350 mitochondrial membrane potential very directly, but also for quantitative detection,
351 because the degree of mitochondrial depolarization can be measured by the ratio of
352 red/green fluorescence intensity. From the experimental results, it was observed that
353 the JC-1 staining changed from red to green with the increase of temperature,
354 suggesting that the mitochondrial membrane potential depolarization was serious at
355 high temperature, and the membrane potential decreased and apoptosis occurred in the
356 cells.

357 ROS is a class of single-electron reduction products of oxygen in the body,
358 which are generated by leaking electrons out of the oxidative respiratory chain and
359 consuming about 2% of the oxygen before it is passed to the terminal oxidase,
360 including the one-electron reduction product of oxygen, superoxide anion, two-
361 electron reduction product, hydrogen peroxide, three-electron reduction product,
362 hydroxyl radical, and nitric oxide. ROS production is mainly formed by the high
363 oxygen environment and the high reduced state of the respiratory chain in the
364 mitochondrial transition from state III to state IV, which causes a large number of
365 electrons to leak out and reduce oxygen molecules. Under pathological conditions, the
366 loss of the normal balance between the production and removal of ROS often results
367 in damage to the body by ROS. Oxidative damage mainly includes: first, oxidative
368 damage to nucleic acids, after oxidative damage to the DNA may occur breaks,
369 mutations and changes in thermal stability, which seriously affects the normal
370 transcription and translation of genetic information; second, modification of amino
371 acids, peptide chain breaks, the formation of cross-linked polymers of proteins,
372 changes in conformation and immunogenicity, and other five aspects. Most of the
373 hydroxyl radicals in the organism are produced in the organelles, especially in the
374 mitochondria, causing damage to the mitochondrial membrane and leading to
375 impaired energy metabolism in the cells and the organism ^[21-22]. The present study
376 showed that with increasing temperature, mitochondrial oxidative stress ROS content
377 increases, demonstrating increased production and release of mitochondrial oxides
378 and inhibited activity.

379 The results of ROS and JC- 1 assays were in line with the mechanistic studies in
380 humans when heat stroke occurs, such as in heat stroke, cells in the body are in a

381 hypoxic state, ATP is reduced, Ca²⁺ concentration is increased, followed by elevated
382 ROS and oxidative stress, leading to apoptosis, tissue necrosis and autophagy, and
383 eventually multi-organ dysfunction and individual death [23-24]. Interestingly, the
384 results in this experiment showed that ROS was elevated and mitochondrial activity
385 was reduced when hADSCs cells were in a high temperature environment; the cell
386 membrane depolarization was severe during JC-1 staining, which may also lead to
387 dysregulation of Ca²⁺ flow. It may further explain that when people are under high
388 temperature all the time, the growth of hADSCs cells is restricted and cellular
389 oxidative stress is severe, and then apoptosis or cell death occurs, resulting in the loss
390 of the ability of adipocytes to maintain body temperature, and the final trend is the
391 loss of organismal function and death.

392 ADSCs are widely distributed in vivo, including subcutaneous tissues. The
393 changes in cellular activity and function of hADSCs induced by high temperature are
394 closely related to explain the aging of epidermal cells, dysregulation of lipid
395 metabolism and maintenance of body temperature. Therefore, we hypothesize that
396 humans and animals growing near the equator or in hot regions are affected by high
397 temperatures, which may cause aging of surface cells such as skin in mild cases and
398 impairment of metabolism of cells, tissues and organs in the body in severe cases,
399 thus causing various diseases.

400 In conclusion, hADSCs grown under high temperature conditions have restricted
401 growth activity, blocked S and G2 phases resulting in reduced cell division, enhanced
402 osteogenic differentiation, impaired mitochondrial activity, and severe cell
403 depolarization. These phenomena are directly related to skin aging, apoptosis and heat
404 stroke diseases caused by outdoor exposure to sunlight in summer as reported by
405 previous researchers. These results may provide a further explanation for global
406 warming to localize high temperatures, causing the cause of species extinction.

407

408 **Abbreviations**

409 hADSCs: human adipose-derived mesenchymal stromal cells; ROS: Reactive oxygen
410 species.

411

412 **Acknowledgments**

413 The authors thank all students and technicians in the laboratory for their cooperation.

414

415 **Author's Contributions**

Yuanhui Gao	performed experiments, provided funding supported
Hui Cao	performed experiments
Shunlan Wang	performed experiments
Linlin Zheng	performed experiments
Haowei He	performed experiments
Zhenyu Nie	helped with the experiments
Mei Chen	helped with the experiments
Rong Jiang	discussed with clinical disease
Denggao Huang	provided funding supported, provided the expert opinion in temperature design, co-wrote and finalized the manuscript text, monitored the research design and progress
Shufang Zhang	provided funding supported, monitored the research design and progress

416

417 **Funding**

418 This research was supported by the Hainan Provincial Natural Science Foundation of
419 China (819QN386, 819QN390, ZDKJ2017007)

420

421 **Availability of data and materials**

422 The data that support the findings of this study are available from the corresponding
423 author upon request.

424

425 **Ethics approval and consent to participate**

426 Not applicable.

427

428 **Consent for publication**

429 Not applicable.

430

431 **Competing interests**

432 The authors declare that they have no competing interests.

433

434 **Author information**

435 ¹Department of Central Laboratory, Afliated Haikou Hospital of Xiangya Medical
436 College, Central South University, Haikou 570208, Hainan, China
437 ²Department of General Surgery, 900th Hospital of the Joint Logistics Team/Clinical
438 Institute of Fuzhou General Hospital, Fujian Medical University/Dongfang Hospital
439 Affiliated of Xiamen University, Fuzhou 350025, Fujian, China

440
441

442 **References**

- 443 [1] Jeremy M Cohen, Erin L Sauer, Olivia Santiago, Samuel Spencer, Jason R Rohr. Divergent
444 impacts of warming weather on wildlife disease risk across climates. *Science*. 2020, 370(6519):
445 eabb1702.
- 446 [2] Christopher H Trisos, Cory Merow, Alex L Pigot. The projected timing of abrupt ecological
447 disruption from climate change. *Nature*. 2020, 580(7804): 496- 501.
- 448 [3] Ken Kobayashi, Yusaku Tsugami, Kota Matsunaga, Takahiro Suzuki, Takahiro Nishimura.
449 Moderate High Temperature Condition Induces the Lactation Capacity of Mammary Epithelial
450 Cells Through Control of STAT3 and STAT5 Signaling. *J Mammary Gland Biol Neoplasia*.
451 2018 Jun;23(1-2):75-88.
- 452 [4] Torlińska T, Banach R, Paluszak J, Gryczka-Dziadecka A. Hyperthermia effect on lipolytic
453 processes in rat blood and adipose tissue. *Acta Physiol Pol*. 1987, 38(4):361-6.
- 454 [6] Qi Zhao, Yuming Guo, Tingting Ye, et al. Global, regional, and national burden of mortality
455 asso ciated with non-optimal ambient temperatures from 2000 to 2019: a three-stage modelling
456 study. *Lancet Planet Health*. 2021, 5(7): e415-e425.
- 457 [7] A. Bouchama and J. P. Knochel. Heat stroke. *N Engl J Med*. 2002, 346(25): 1978-1988.
- 458 [8] Lu Kuo-Cheng, Wang Jia-Yi, Lin Shih-Hua, et al. Role of circulating cytokines and
459 chemokines in exertional heatstroke. *Critical care medicine*, 2004, 32(2): 399-403.
- 460 [9] María E Frigolet, Ruth Gutiérrez-Aguilar. The colors of adipose tissue. *Gac Med Mex*. 2020;
461 156(2):142-149.
- 462 [10] Ziad Obermeyer, Jasmeet K Samra, Sendhil Mullainathan. Individual differences in normal
463 body temperature: longitudinal big data analysis of patient records. *BMJ*. 2017, 359: j5468.
- 464 [11] Michael Gurven, Thomas S Kraft, Sarah Alami, Juan Copajira Adrian, et al. Rapidly
465 declining body temperature in a tropical human population. *Sci Adv*. 2020, 6(44): eabc6599.
- 466 [12] Chi Xu, Timothy A Kohler, Timothy M Lenton, Jens-Christian Svenning, Marten Scheffer.
467 Future of the human climate niche. *Proc Natl Acad Sci U S A*. 2020,117(21):11350-11355.
- 468 [13] Symonds ME, Aldiss P, Dellschaft N, Law J, Fainberg HP, Pope M, Sacks H, Budge H.
469 Brown adipose tissue development and function and its impact on reproduction. *J Endocrinol*.
470 2018, 238(1): R53-R62.
- 471 [14] Ludovic Zimmerlin, Vera S Donnenberg, J Peter Rubin, Albert D Donnenberg. Mesenchymal

472 markers on human adipose stem/progenitor cells. *Cytometry A*. 2013, 83(1):134-40.

473 [15] Alexander Mildmay-White, Wasim Khan. Cell Surface Markers on Adipose- Derived Stem
474 Cells: A Systematic Review. *Curr Stem Cell Res Ther*. 2017, 12(6): 484-492.

475 [16] Ting Jiang, Wei Liu, Xiaojie Lv, Hengyun Sun, Lu Zhang, Yu Liu, Wen Jie Zhang, Yilin Cao,
476 Guangdong Zhou. *Biomaterials*. 2010, 31(13):3564-71.

477 [17] Imran Ullah, Raghavendra Baregundi Subbarao, Gyu Jin Rho. Human mesenchymal stem
478 cells - current trends and future prospective. *Biosci Rep*. 2015,35(2): e00191.

479 [18] Sue Im Jang, Myeongryeol Lee, Yu Chul Jung, Min Kyung Jeong, Ja Hyun Ryu , Beom Joon
480 Kim, Byung-Fhy Suh, Eunjoo Kim. Skin characteristics following repeated exposure to
481 simulated outdoor and indoor summer temperatures in South Korea and Southeast Asia. *Int J*
482 *Cosmet Sci*. 2021,17.

483 [19]S Kim, J W Park, Y Yeon, J Y Han, E Kim. Influence of exposure to summer environments on
484 skin properties. *J Eur Acad Dermatol Venereol*. 2019, 33(11): 2192- 2196.

485 [20] Tatiana K Rostovtseva, Wenzhi Tan, Marco Colombini. On the role of VDAC in apoptosis:
486 fact and fiction. *J Bioenerg Biomembr*. 2005, 37(3):129-42.

487 [21] Jakubczyk K, Dec K, Kałduńska J, Kawczuga D, Kochman J, Janda K. Reactive oxygen
488 species - sources, functions, oxidative damage. *Pol Merkur Lekarski*. 2020, 48(284):124-127.

489 [22] Tan DQ, Suda T. Reactive Oxygen Species and Mitochondrial Homeostasis as Regulators of
490 Stem Cell Fate and Function. *Antioxid Redox Signal*. 2018, 29(2):149-168.

491 [23] Sheng-Hsien Chen, Mao-Tsun Lin, Ching-Ping Chang. Ischemic and oxidative damage to the
492 hypothalamus may be responsible for heat stroke. *Curr Neuropharmacol*. 2013, 11(2):129-40.

493 [24] Hsin-Hsueh Shen, Yu-Shiuan Tseng, Ni-Chun Kuo, et al. Alpha-Lipoic Acid Protects
494 Cardiomyocytes against Heat Stroke-Induced Apoptosis and Inflammatory Responses
495 Associated with the Induction of Hsp70 and Activation of Autophagy. *Mediators Inflamm*.
496 2019, 2019: 8187529.